P1.81 CHARACTERISTICS OF CLOUDS AND PRECIPITATION OVER THE PACIFIC COAST OF SOUTHERN MEXICO RETRIEVED FROM THE TRMM SATELLITE PRODUCTS

Beata Kucienska[1] and G. B. Raga

Centro de Ciencias de la Atmósfera, Universidad Nacional Autónoma de México

1. INTRODUCTION

The southern Mexican states located close to the Pacific coast are affected by intense precipitation that develops as a consequence of large-scale meteorological conditions, breezes resulting from a land-sea thermal contrast and mountain ranges which enhance rainfall due to valley breezes and orographic uplift. An important topographic feature of the studied region is a 40 km gap in the mountain range located in the central part of the Isthmus of Tehuantepec. The strengthening of the offshore jet in this gap during July and August contributes to the occurrence of mid-summer drought observed in this region (Romero-Centeno et al. 2007). In late July and early August rainfall amounts fall by 40%, as compared to those of June and September (Magaña et al. 1999). The strengthening of the Tehuantepec jet during midsummer is caused by an increase of the sea-level pressure difference between the western Atlantic and the eastern Pacific, which is induced by the penetration of the Azores-Bermuda high into the Gulf of Mexico (Romero-Centeno et al. 2007).

The eastern Pacific pool located off the west coast of southern Mexico is characterized by sea surface temperatures above 27°C and it is a zone where tropical cyclones develop. The studied region is also influenced by the intertropical convergence zone.

Precipitating clouds in the tropics are convection-generated cumulonimbi (Houze 1997). When cumulonimbus clouds develop over the coast, diurnal evolution of precipitation is affected by the land-sea breeze pattern. In this paper we analyze temporal and spatial evolution of rainfall over the land and ocean zones and its relation to the diurnal evolution of land and sea breezes measured by Baumgardner et al. (2006) in this region.

The data analyzed in this study come from the Precipitation Radar, Microwave Imager and Visible and Infrared Scanner on the satellite of the Tropical Rainfall Measuring Mission (TRMM), which is a joint mission between the National Aeronautics and Space Administration of the United States and The National Space Development Agency of Japan. The objectives of TRMM are to measure rainfall and energy exchange of tropical and subtropical regions of the world (Kummerow et al. 1998). The TRMM satellite was launched on 27th November 1997 into an inclined orbit extending between 35°N and 35°S at 350-km altitude and boosted to an altitude of 402 km in August 2001. TRMM's Precipitation Radar is the first radar designed to monitor rainfall from space.

The analyzed average diurnal evolution of precipitation covers a 12-year period (1998-2009) and it is obtained from the data of 3B42 TRMM product. In order to understand the nature of the rainfall over the region of interest, an analysis of hydrometeor profiles retrieved from 2A12 TRMM product has been done.

In addition to precipitation climatology, the spatial and temporal evolution of lightning is analyzed. The lightning data for the period 2006-2009 come from the World Wide Lightning Location Network

[1] Corresponding author e-mail: beata@atmosfera.unam.mx

(WWLLN) and are compared with the data registered by TRMM Lightning Imaging Sensor (LIS) and the Optical Transient Detector (OTD) on the MicroLab-1 satellite.

2. METHODOLOGY

The studied region is located between the parallels 12^{o}N and 18^{o}N and meridians 93^{o}W and 101^{o}W. Its location is shown in the Fig. 1a. In order to compare the precipitation over land and ocean, the region was divided in two zones: ocean zone (latitude: 12N - 15N) and land zone (latitude: 15N - 18N). The land zone is characterized by high mountains and a 40 km gap between two mountain ranges located in the central part of the Isthmus of Tehuantepec. Its topography is shown in the Fig. 1b.

Figure 1a. Location of the studied region.

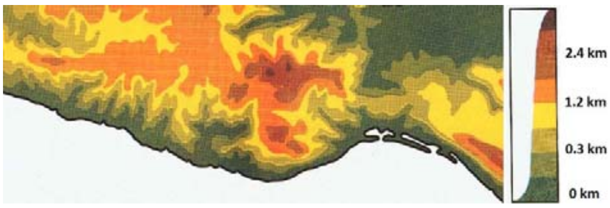

Figure 1b. Topographic map of the studied zone

The data retrieved from the TRMM satellite products 3B42 and 2A12 are used to analyze the diurnal evolution and spatial distribution of precipitation and the characteristics of hydrometeor profiles over the Pacific coast of southern Mexico. The 12-year precipitation climatology is compared with the lightning data registered by the World Wide Lightning Location Network during 4 years. The WWLLN data are verified against a LIS/OTD climatologic product HRMC (High Resolution Monthly Climatology).

3. RESULTS

3.1. Diurnal evolution and spatial distribution of precipitation

The pattern of diurnal evolution and spatial distribution of precipitation is very similar for the four summer months (June to September). In the Fig. 2 a diurnal cycle of September precipitation, averaged over 12 years, is presented. Spatially-averaged, 3-hour accumulated rainfall, calculated for all the months of the year, is shown in Fig. 3a (land zone) and 3b (ocean zone). September is the month when the rainfall amounts are largest for both land and ocean zones, but the reduction of rainfall during July and August (as compared to June rainfall) is more pronounced over the ocean zone.

Below we analyze the influence of sea and land breezes measured by Baumgardner et al. (2006) at the coastal town of Salina Cruz on the diurnal evolution of precipitation over land and ocean zones, registered by TRMM sensors.

- A minimum summer rainfall over land is observed at midday. At the same hour a reversal in wind direction occurs: land breeze is replaced by sea breeze which starts to bring humid air to the coast.
- At 3pm strong convective motions begin to saturate upper atmosphere with water vapor. The combined effects of atmospheric convection, sea and valley breezes and orographic uplift result in the development of cumulonimbus clouds over the land.
- The maximum frequency of sea breeze events was observed at 5pm (Baumgardner et al. 2006) therefore the maximum moisture flux toward the coastline is expected to occur in late afternoon hours. However the maximum rainfall over land was registered between 9pm and midnight (Fig. 3a). It takes several hours before hot, tropical air becomes saturated and the resulting precipitation is a long-lasting one: it continues until morning.
- The minimum precipitation over ocean zone coincides with the maximum rainfall over land: it occurs about 9pm (Fig. 2 and 3). The sea breeze is replaced by a land breeze after 10pm.
- The land breeze provokes sinking motions of the air over ground. After midnight rainfall over land zone decreases (Fig. 3a). At the same time the precipitation over ocean zone starts to increase (Fig. 3b) and at 3am there is more rainfall over sea than over land. The maximum frequency of land breeze was observed at 6am and this is also the hour when the maximum rainfall over ocean is registered.
- Between 6am and noon the precipitation over sea decreases slightly but is still significant and extends along the whole coastline (Fig. 2). Meanwhile land rainfall approaches its minimum. In the morning a strong precipitation gradient across the coastline can be noticed (Fig. 2).

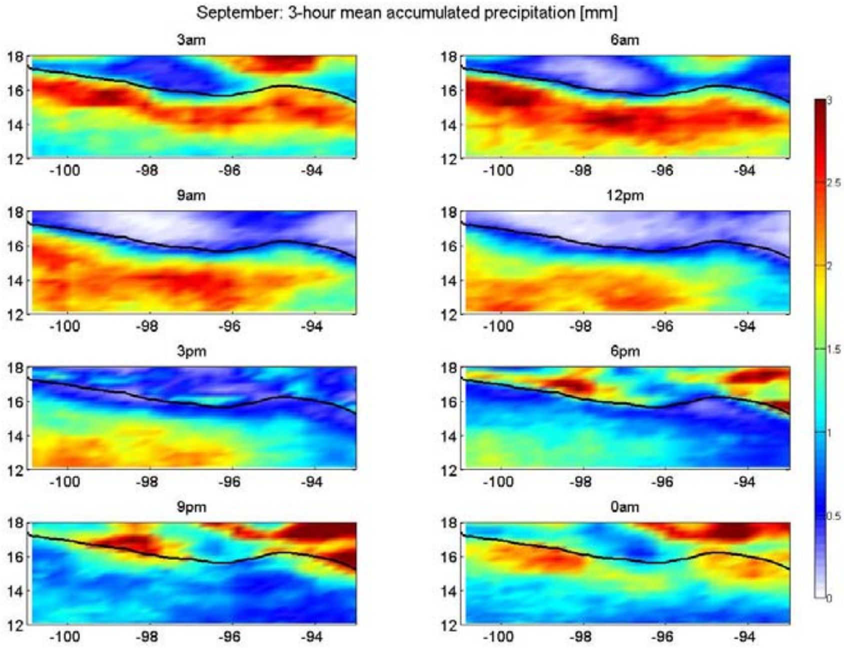

Figure 2. Three-hour mean accumulated precipitation in September. The data are averaged over 12 years: 1998-2009.

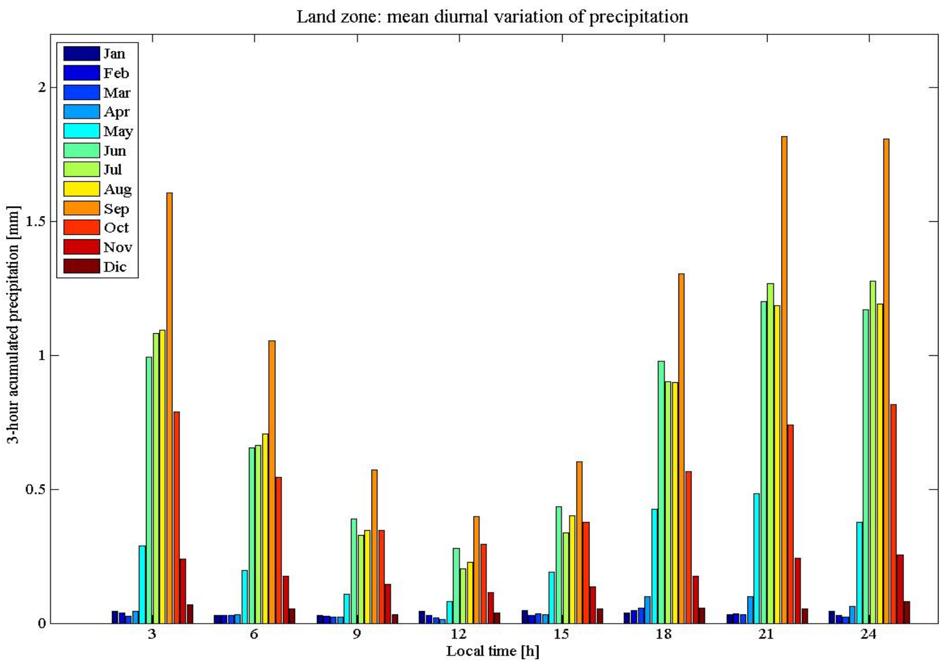

Figure 3a. Spatial average of accumulated precipitation for the land zone. The 3-hour averages are centered at the hours indicated in the figure

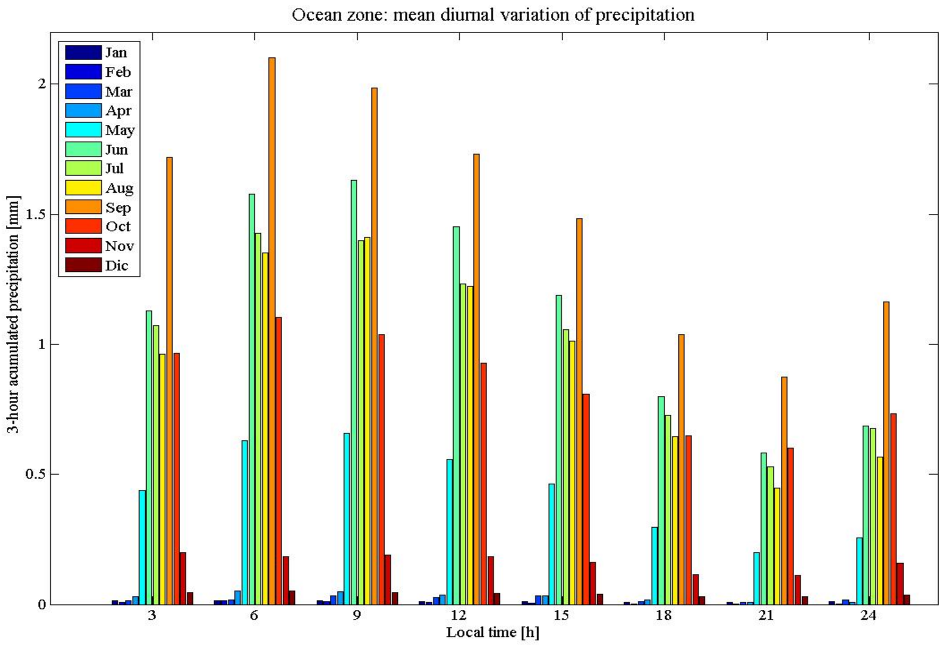

Figure 3b. The same as in the Fig. 3a, but for the ocean zone.

3.2. Vertical hydrometeor profiles

The vertical profiles of hydrometeors were retrieved for the year 2008 when La Niña - Southern Oscillation event was registered over Tropical Pacific, (http://www.esrl.noaa.gov/psd/people/klaus.wolter/MEI/table.html).

Spatial averages are calculated for land and ocean zones and temporal averages are considered for daytime (between 6am and 6pm) and night (between 6pm and 6am). The results are presented in the Fig. 4 and 5. Water content in precipitating clouds over land is larger during night than during day and the opposite situation occurs for the ocean zone. This result is consistent with the surface precipitation data retrieved from 3B42 TRMM product.

The maximum amount of precipitating ice, as calculated by the TRMM 2A12 algorithm, is located at 6 km above the surface and its value is very close to that of precipitating water at the lowest level (0.5 km), which indicates that the origin of summer precipitation is melted ice for both land and sea zones.

The shapes of vertical profiles of precipitating ice are different for ocean and land zones. In case of the ocean there is a layer with an almost constant amount of precipitating ice between 6 km and 8 km, whereas over the land zone there is a clear maximum of precipitating ice at 6 km. The differences in the profiles of hydrometeors for land and ocean zones are most likely caused by different size distributions of cloud condensation nuclei and ice nuclei.

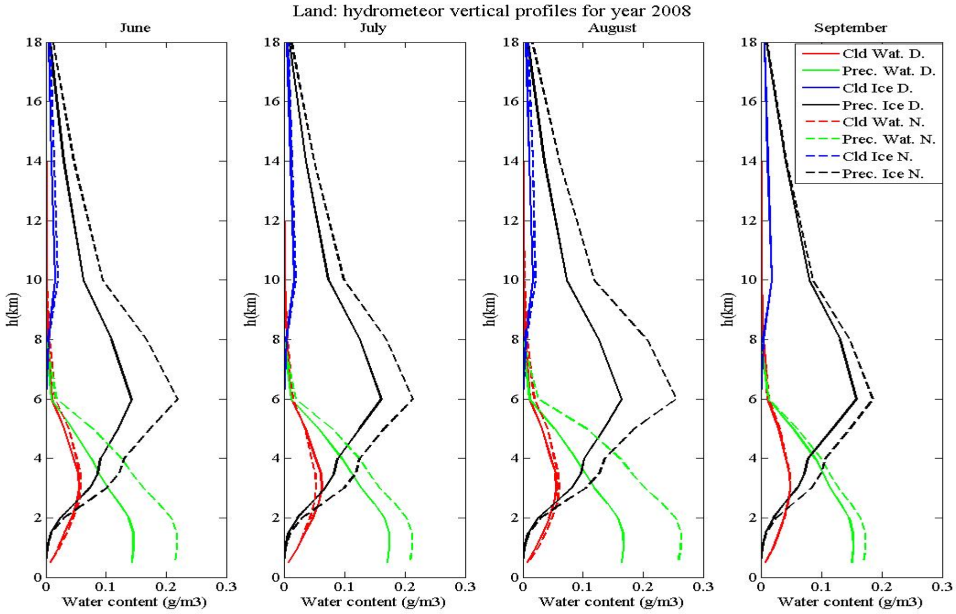

Figure 4. Vertical hydrometeor profiles over land zone in 2008, for months June, July, August and September. Solid lines represent day average and dashed lines night average.

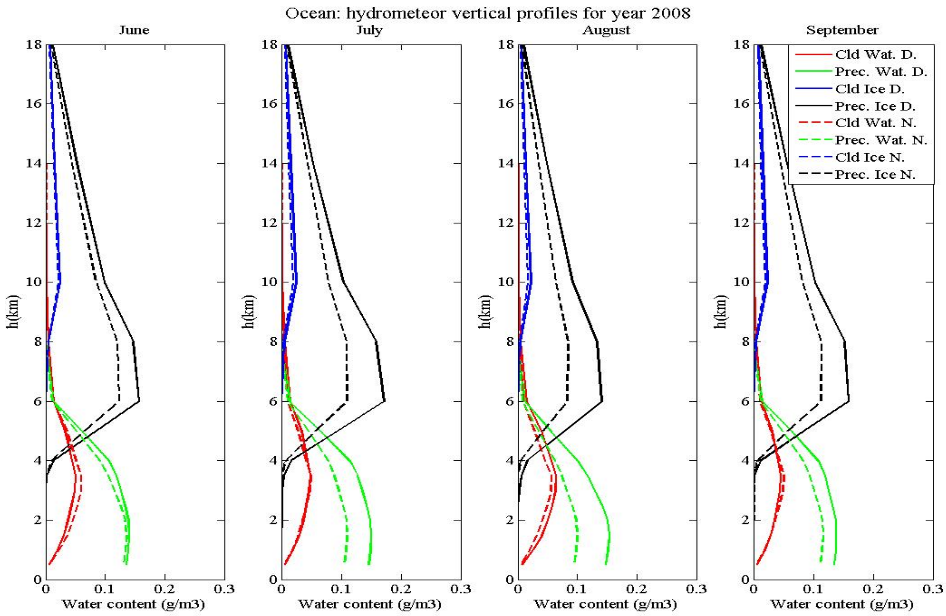

Figure 5. The same as in the Fig. 4, but for the ocean zone.

3.3 Diurnal evolution and spatial distribution of lightning

The diurnal evolution of lightning strokes to ground for September, averaged over 12 years, is presented in Fig. 6. Spatially-averaged, 3-hour accumulated flashes, calculated for all months of the year, are shown in Fig.7a (land zone) and 7b (ocean zone).

In general, spatial patterns of lightning density are similar to those of rainfall (compare Fig. 2 and 6) however there are some lightning features that do not coincide with the temporal variation of precipitation:

- There is a very high concentration of strokes at the southern side of the coastline between midnight and 3am (Fig. 6). The maximum number of strokes in this area is not in phase with the maximum rainfall, which is observed at 6am (Fig. 2).
- September is the month with the highest rainfall for both land and ocean zones (Fig. 3a and 3b), however the situation is different for the lightning density. Over the ocean zone there are more flashes during August than during September at any hour (Fig. 7b) and over the land zone the number of registered strokes is similar for both months (although slightly higher in August) before midday. From 3pm until midnight there are more flashes registered in September than in August over the land zone.
- Over the ocean zone rainfall in June is more than twice greater than that of May, at any hour, and it is also considerably greater than that of July (Fig. 3b), however there are more lightning strokes both in May and July than in June (except at the hours 9pm and 0am when there is slightly smaller lightning concentration in May than in June), as shown in the Fig. 7b.

In order to confirm the validity of the data provided by the World Wide Lightning Location Network we use climatologic data from LIS/OTD gridded product HRMC (High Resolution Monthly Climatology). Monthly variation of lightning strokes, as registered by the WWLLN, is shown in the Fig. 8a and the data registered by OTD and LIS sensors are shown in the Fig. 8b. There is a difference of one order of magnitude between the WWLLN and LIS/OTD data. This is understandable when one considers that the WWLLN detects only cloud to ground lightning with an efficiency of about 30%, whereas LIS detects total lightning and its efficiency is above 90%.

The LIS/OTD data confirm the WWLLN records which reveal that there are less lightning strokes in June than in May and July, and more flashes occur in August than in September over the ocean zone. Both WWLLN and LIS/OTD data exhibit a bimodal monthly distribution of flashes for the ocean zone and a unimodal one for the land zone. In case of the ocean zone both datasets reveal the lightning maxima in May and August, however the maximum registered by WWLLN over the land zone occurs in September and that of LIS/OTD in August. This discrepancy can be explained if one considers that the proportion between cloud to ground strokes (registered by WWLLN) and total lightning (LIS/OTD HRMC product) can vary throughout the year.

The analysis of lightning data demonstrates that the cumulonimbi which produce the greatest rainfall over the studied region do not generate the highest number of lightning strokes. The explanation of this finding should include the analysis of microphysical processes which is beyond the scope of this study. A possible explanation can be related to the amount of supercooled cloud water which plays an important role in the process of charge separation. However, the hydrometeor profiles retrieved from 2A12 TRMM product (Fig. 4 and 5) do not provide evidence for a considerable difference in the amount of cloud water for months with low and high flash rate density. Further study of this topic should provide more insight into that issue.

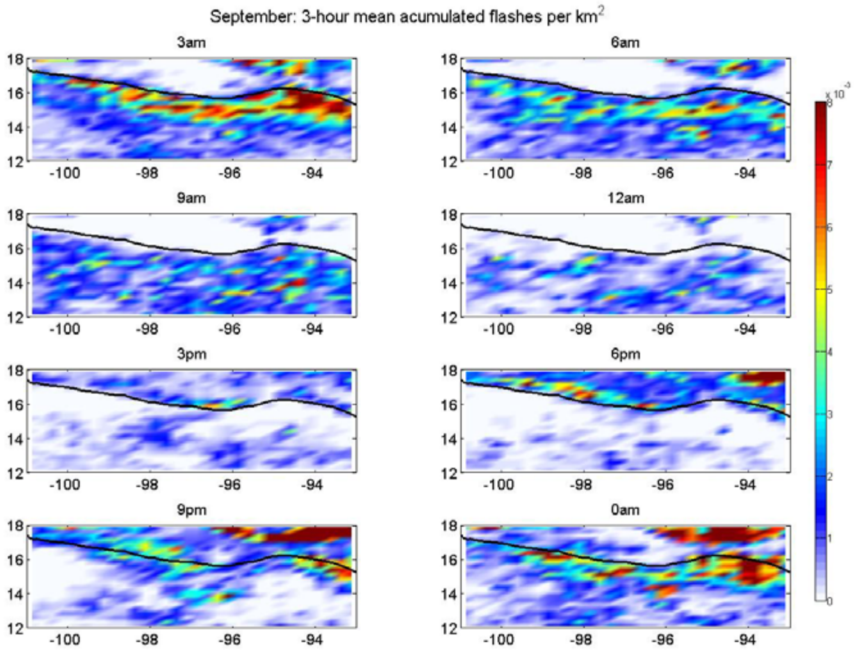

Figure 6. Three-hour mean accumulated flashes per km^2 in September. The data are averaged over 4 years: 2006-2009.

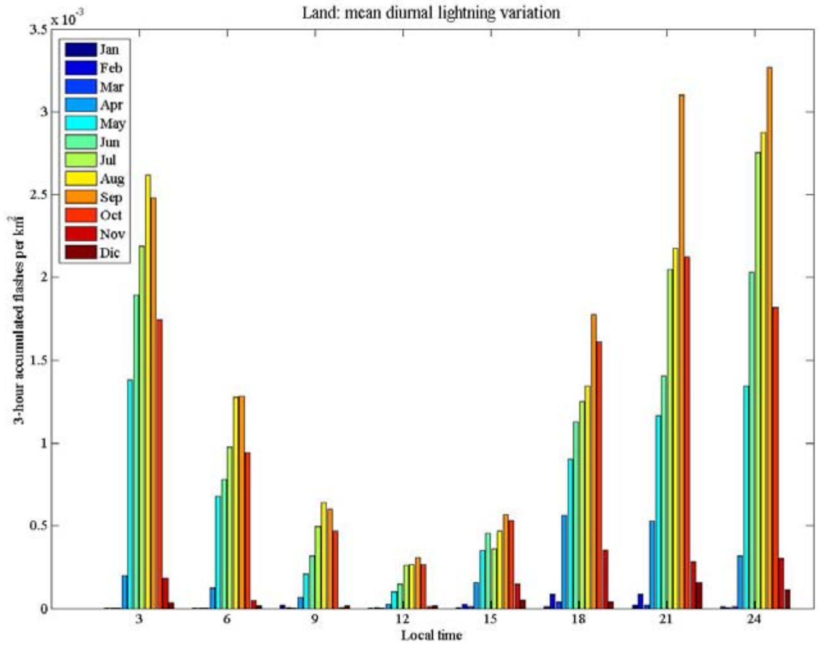

Figure 7a. Spatial average of lightning strokes surface density for the land zone. The 3-hour averages are centered at the hours indicated in the figure.

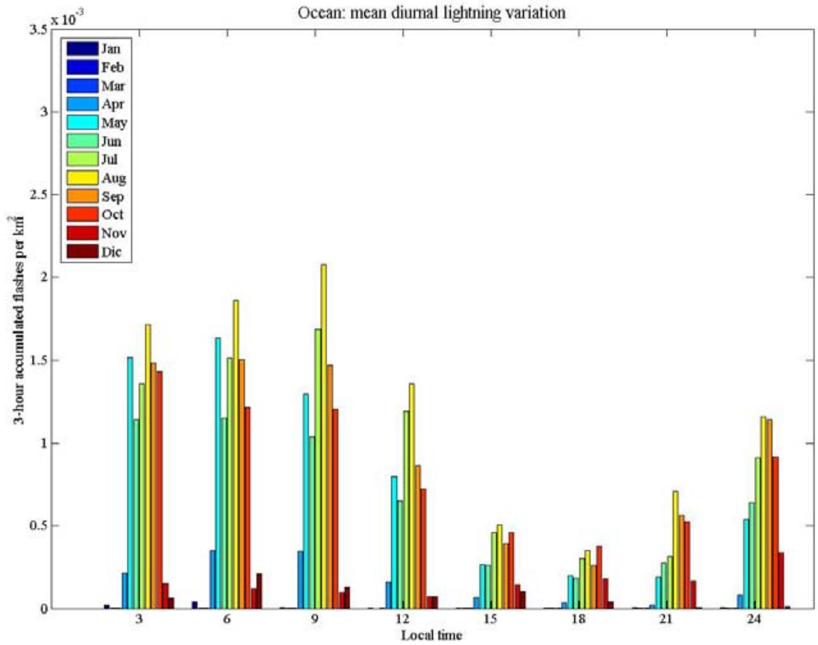

Figure 7b. The same as in the Fig. 7a, but for the ocean zone.

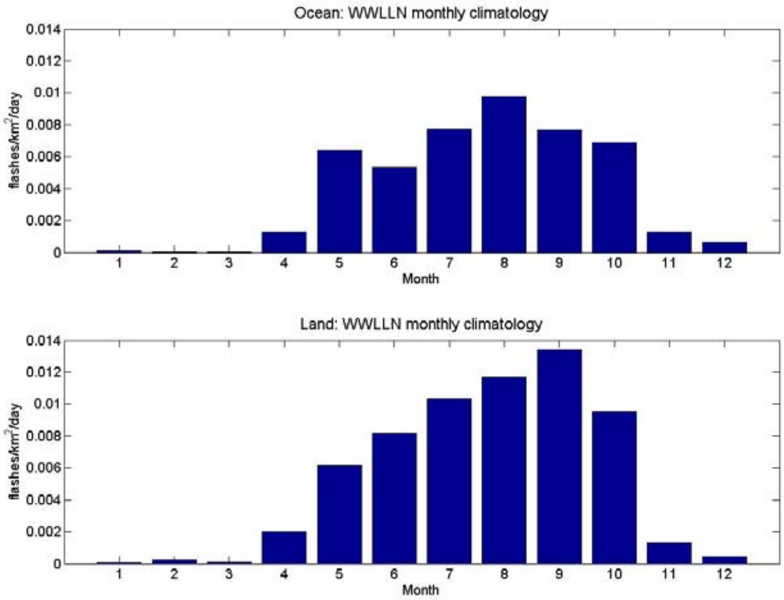

Figure 8a. Monthly climatology of lightning strokes for ocean and land zones retrieved from the WWLLN data.

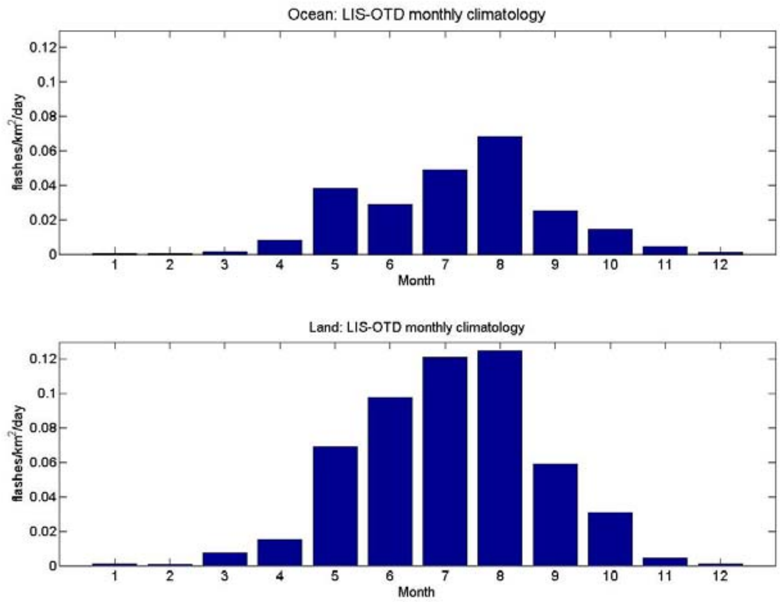

Figure 8b. Monthly climatology of lightning strokes for ocean and land zones retrieved from the LIS-OTD gridded product HRMC.

4. SUMMARY AND CONCLUSIONS

In the present study the climatology of precipitation and lightning over the Pacific coast of southern Mexico is retrieved from the TRMM products. The WWLLN data are used to analyze the spatial distribution of lightning.

Both 3B42 and 2A12 TRMM datasets prove that the summer rainfall over land is greater during night than during day and the opposite situation occurs for the ocean zone. The precipitation over the studied zone follows the breeze cycle and therefore its maximum occurs at night over the land and in the morning over the ocean.

The hydrometeor profiles retrieved from the 2A12 TRMM product reveal that the maximum amount of precipitating ice is almost the same as that of precipitating water, which means that the summer precipitation over the studied zone is the result of mixed phase processes.

The spatial distribution of lightning is similar to that of rainfall: the areas with intense rainfall coincide with those that exhibit large number of strokes. However there is a phase shift of several hours between the maximum rainfall and the maximum lightning density over the ocean area near the coastline.

Both WWLLN and LIS/OTD data reveal a bimodal monthly distribution of flashes for the ocean zone and a unimodal one for the land zone. The monthly variation of lightning stroke density does not coincide with that of rainfall, especially over the ocean, where the summer months with maximum rainfall (June and September) exhibit a low number of flashes and those that correspond to mid-summer drought (June and August) have much higher lightning density. This discrepancy is an issue which needs to be investigated.

Acknowledgements: This study was carried out with support from Semarnat-Conacyt grants 23498 and 23499.

REFERENCES

Adler, R. F., Huffman G. J., and Keehn P. R., 1994, Global tropical rain estimates from microwave-adjusted geosynchronous IR data. *Remote Sens. Rev.,* **11,** pp. 125–152

Baumgardner D., Raga G. B., Grutter M. and Lammel G, 2006, Evolution of anthropogenic aerosols in the coastal town of Salina Cruz, Mexico: Part I particle dynamics and land-sea interactions. *Sci. Tot. Env.,* **367**, pp. 288-301.

Christian, H. J., Blakeslee R. J., Boccippio D. J., Boeck W. L., Buechler D. E., Driscoll K. T., Goodman S. J., Hall J. M., Koshak W. J., Mach D. M., and Stewart M. F., 2003, Global frequency and distribution of lightning as observed from space by the Optical Transient Detector. *J. Geophys. Res.*, **108(D1)**, 4005, doi:10.1029/2002JD002347.

Houze, R.A. Jr., 1997, Stratiform precipitation in regions of convection: A meteorological paradox? *Bull. Amer. Meteor. Soc.*, **78**, pp. 2179-2196.

Kummerow C, Olson W.S. and Giglio L., 1996, A simplified scheme for obtaining precipitation and vertical hydrometeors profiles from passive microwave sensors. *IEEE Trans. on Geosci. and Remote Sensing*, **34**, pp. 1213-1232.

Kummerow C. and Barnes W., 1998, The Tropical Rainfall Measuring Mission (TRMM) sensor package. *J. Atmos. Oceanic Technol.,* **15,** pp. 809–816.

Kummerow C., Simpson J., Thiele O., Barnes W., Chang A.T.C., Stocker E., Adler R.F., Hou A., Kakar R., Wentz F., Ashcroft P., Kozu T., Hong Y., Okamoto K., Iguchi T., Kuroiwa H., Im E., Haddad Z., Huffman G., Ferrier B., Olson W.S., Zipser E., Smith E.A., Wilheit T.T., North G., Krishnamurti T., and Nakamura K**,** 2000, The status of the Tropical Rainfall Measuring Mission (TRMM) after two years in orbit*. J. of Appl. Meteorol.*, **39**, pp. 1965-1982.

Magaña, V., Amador J., and Medina S., 1999, The midsummer drought over Mexico and Central America. *J. Climate*, **12**, pp. 1577–1588.

Montero-Martínez, G., Zarraluqui-Such V., Caetano E. S., and García-García F., 2010, Hydrometeor vertical characterization of precipitating clouds over the Mexico Basin. *International Journal of Remote Sensing.* In press*.*

Rodger, C. J., Brundell J. B., and Dowden R. L., 2005, Location accuracy of VLF World Wide Lightning Location (WWLL) network: Post-algorithm upgrade*. Ann. Geophys.*, **23**, pp. 277-290.

Romero-Centeno R, Zavala-Hidalgo J and Raga G.B., 2007, Midsummer gap winds and low-level circulation over the eastern tropical Pacific. *J. Climate*, **20**, pp. 3768–84.